DEVELOPMENT OF A NEW LATERAL STABILITY CONTROL SYSTEM ENHANCED WITH ACCELEROMETER BASED TIRE SENSORS

Gurkan Erdogan
Francesco Borrelli
Department of Mechanical Engineering
University of California, Berkeley
Berkeley, CA 94720-1740
gurkan@berkeley.edu
fborrelli@berkeley.edu

Riccardo Tebano
Giorgio Audisio
Pirelli Tyre SpA
Milan 20126, Italy
riccardo.tebano@pirelli.com
giorgio.audisio@pirelli.com

Giulia Lori
Jacopo Sannazzaro
Department of Mechanical Engineering
Politecnico Di Milano
Milan 20156, Italy
giulia.lori@mail.polimi.it
jacopo.sannazzaro@mail.polimi.it

ABSTRACT

Vehicles are usually equipped with driver assistance systems such as anti-lock brake, traction control and lateral stability control systems. Although the forces maneuvering a vehicle are generated inside the tire contact patch, state of the art control systems have no feedback directly from the tires. Instead, observers based on indirect measurements are employed to close the control loop.

Wireless sensors embedded inside the tires can be used to extract valuable information from the tire deformations such as forces. These forces can be used to develop adaptive stability control systems which update their parameters in real-time depending on the road and vehicle conditions. Furthermore, controllers can selectively regulate tire forces by changing brake/drive torques at each tire.

This paper examines the integration of accelerometer based tire sensors with lateral stability control system (ESP). Its aim is to present the main components of a smart-tire enabled ESP and a preliminary study on potential performance improvements.

NOMENCLATURE:

CoG	Center of gravity
a, b	Distances of CoG from the front and rear axles [m]
c	Half track width [m]
r	Effective radius of the wheel[m]
I_v	Vehicle mass moment of inertia in z-axis [kgm^2]
I_w	Wheel and driveline mass moment of inertia [kgm^2]
m	Vehicle mass [kg]
i	Index for indicating front and rear: $i=\{F,L\}$
j	Index for indicating left and right: $j=\{L,R\}$
$F_{x\,ij}$	Longitudinal tire forces in the vehicle body frame [N]
$F_{y\,ij}$	Lateral tire forces in the vehicle body frame [N]
$F_{l\,ij}$	Longitudinal tire forces in the wheel body frame [N]
$F_{c\,ij}$	Lateral tire forces in the wheel body frame [N]
$v_{x\,ij}$	Long. wheel velocities in the vehicle body frame [m/s]
$v_{y\,ij}$	Lateral wheel velocities in the vehicle body frame [m/s]
$v_{wx\,ij}$	Long. wheel velocities in the wheel body frame [m/s]
$v_{wy\,ij}$	Lateral wheel velocities in the wheel body frame [m/s]
F_{drag}	Drag force acting on the vehicle [N]
F_{roll}	Total rolling resistance acting on the vehicle [N]

$T_{Brk\,ij}$	Brake torques for each tire [Nm]
$\mathbf{R}$	Coordinate transformation matrix
$k_{roll\,i}$	Front and rear suspension stiffness [N/m]
v_{CoG}	Speed of vehicle *CoG* [m/s]
g	Gravitational acceleration [m/s^2]
a_x	Long. Acceleration of the vehicle in inertial frame [m/s^2]
a_y	Lat. Acceleration of the vehicle in inertial frame [m/s^2]
$\dot{x}, \dot{y}$	Longitudinal and lateral *CoG* velocities [m/s]
δ_F	Front wheel steering [deg]
$\dot{\psi}$	Yaw rate [rad/s]
ω_{ij}	Wheel angular velocities [rad/s]
$\dot{\omega}_{ij}$	Wheel angular accelerations [rad/s^2]
κ_{ij}	Tire slip ratios [%]
α_{ij}	Tire slip angles [deg]
$F_{z\,ij}$	Normal tire forces [N]
β	Vehicle side slip angle [deg]

INTRODUCTION

The goal of a lateral control system is to stabilize a vehicle in the lateral direction by controlling the yaw rate and the side slip angle. Active front/rear wheels steering [1, 2] and differential wheel braking/driving [3, 4, 5] are the main actuation techniques proposed in the literature for stability control. Various differential braking strategies based on hierarchical control are illustrated in [5]. There, uncoupled SISO controllers along with a supervisor strategy are proposed for guaranteeing the stable and robust behavior. The lateral control system presented in [6] is a model-based MIMO system. The control model is based on a complete four-wheel model in body and inertial coordinate frames. The control input is the steering wheel angle and a GPS receiver is also available onboard. The model presented in [7] is a full vehicle model in body coordinate frame and the control inputs are the variation of longitudinal forces on each tire.

The knowledge of actual and limit traction forces available inside the tire contact patch would be very beneficial independently on the type of control design used. Since the direct measurement of the generated tire forces inside the contact patch is a challenging task, the traditional control systems exploit indirect sensor measurements. A conventional antilock brake system, for example, uses the change in wheel speeds and accelerations as feedback in order not to exceed the maximum available tire forces [24]. Some advanced techniques based on tire slip and force estimations have been proposed in the literature in order to operate the tire in the vicinity of the peak force for minimizing the braking distances These techniques include sliding mode control [8], model predictive control [9] and non-linear PID control [10].

Tire sensors can be used to directly measure the tire slip and the tire forces generated inside the contact patch. Tire sensors based on different technologies have been previously studied in the literature. A surface acoustic wave sensor [11] was proposed to measure the mechanical strains of a tread element inside the contact patch. The sensor is attached to the liner of the tire and a pin is used as a lever and inserted into the tread element from inside the tire for transferring the tread deflections to the sensor's substrate. The capacitive sensor in [12] exploits the similarity between the tire belt structure and an electrical condenser. Tire deformations change the spacing between the steel wires in the tire belt and the sensor measures the capacitance change due to the change in the spacing. The magnetic sensor in [13] is based on the Hall Effect principle. The motion of a magnet embedded into the tire tread induces a potential voltage which is monitored by a Hall sensor. Magnetic sensors are also used to measure the tire sidewall deflections and estimate tire forces [14]. The longitudinal sidewall deformation is picked up by two magnetic field sensors that are mounted to the wheel suspension. The optical sensor consists of an infrared diode, a lens and a position sensitive detector [15]. The diode placed inside the tire emits infrared light which is focused on the detector mounted on the rim by means of the lens. The deflection of the side wall is measured based on the triangulation principle. The main disadvantage of the optical sensor is that the tire carcass can move on the rim after one hard braking and the diode is no longer aligned with the detector. In this paper we propose to use 3D accelerometers embedded inside the tire for the identification of tire deflections and estimation of tire variables [16, 20].

This paper proposes a hierarchical strategy for designing lateral stability control system which use feedback from accelerometer based tire sensors. The high level controller (HLC) determines the amount of brake force necessary for each tire in order to achieve the desired yaw rate and side slip angle, whereas the low level controller (LLC) tries to reach the brake forces requested by the HLC while preventing the saturation of tires. The system employs a PID type of HLC for tracking the yaw rate and slip angle references generated by a bicycle model. The HLC and the LLC are coupled thorough the forces measured by the tire sensors. The interface between the two controllers employs the measured longitudinal tire forces as a feedback in order to control the tire forces more precisely and robustly compared to a traditional open-loop system.

This paper describes the structure of the control system, the integration of the various components and the potential impacts of tire sensors on the design of a lateral stability control system. A simple scenario is used to roughly quantify the potential improvements.

STRUCTURE OF THE CONTROL SYSTEM

The structure of the proposed stability control system is summarized in Fig. 1. The control system is composed of a HLC and a LLC. The HLC regulates the necessary longitudinal tire forces to reach the desired yaw rate and side slip angles while the LLC generates the requested forces using the brake system of the vehicle.

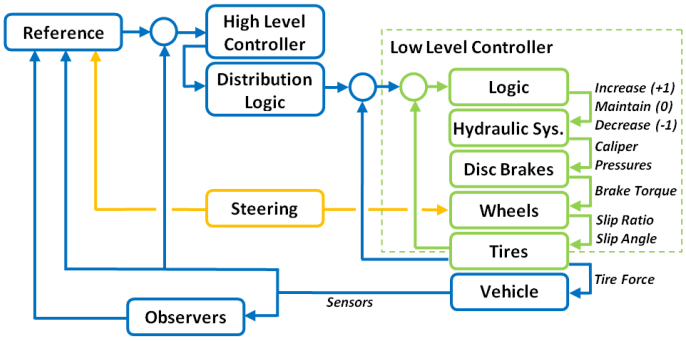

FIGURE 1. OVERALL STRUCTURE OF CONTROL SYSTEM

The HLC is based on two PID controllers which use both yaw rate and side slip angle errors as inputs and generates a torque request which in turn is distributed to the wheels as desired longitudinal forces by using a distribution logic [24]. The LLC tries to track the desired longitudinal forces.

The relationship between the steering wheel angle and the yaw rate of a bicycle model under steady state conditions, also known as Ackerman formula, is used to obtain the yaw rate reference. In Eq.(1), δ is the steering angle, L is the length of the vehicle and ρ is equal to the ratio between the longitudinal velocity, v_x and the characteristic velocity, v_{ch}.

$$\dot{\psi}_{Ack} = \frac{v_x}{1+\rho^2}\frac{\delta}{L} \tag{1}$$

The reference yaw rates are assumed to be saturated and the saturation limits are determined by using the maximum accelerations that a vehicle can achieve without sliding on the roadway. The limits of the vehicle side slip angle are determined as a cubic function of ρ following Eq. (2) [17]. Coefficients of the cubic function k_1, k_2 and k_3 are determined empirically.

$$\beta_{\max} = \begin{cases} 2(k_1-k_2)\rho^3 - 3(k_1-k_2)\rho^2 + k_1 & v_x < v_{ch} \\ k_2 & v_x \geq v_{ch} \end{cases} \tag{2}$$

The LLC, enclosed inside the dotted box in Fig. 1, controls the brake actuators of the vehicle by increasing, decreasing or maintaining the brake caliper pressures depending on the requested longitudinal forces. The brake system is composed of three parts, namely an electronic unit, a hydraulic system and disc brakes. The electronic unit controls the electro-valves and the motor-pump of the hydraulic system to change the pressures activating the brake clamps independent from the driver's brake.

In order to tune the parameters of the hydraulic system, a ABS/ESC test-bench which is a replica of the actual hydraulic system on the test vehicle is employed. During the hardware in the loop (HIL) simulations at different vehicle maneuvers, the caliper brake pressures at each wheel are measured and compared with the pressures requested by the HLC.

The brake torque used in the wheel dynamics are calculated using the Lu-Gre friction model incorporating Stribeck friction phenomena [24]. In Eq. (3), P_{clp} is the caliper pressure, N_{pad} is the number of active pads, A_{pad} is the area of each pad, $v_{relative}$ is the relative velocity between the pad and the brake disc, $v_{stribeck}$ is the Stribeck velocity and R_{pad} is the distance between the pad and the wheel center. A schematic of the disc brake is also presented in Fig. 2.

$$T_{brk} = P_{clp}\, N_{pad}\, A_{pad}\, \mu_{dyn} \tanh\left(\frac{v_{relative}}{v_{stribeck}}\right) R_{pad} \tag{3}$$

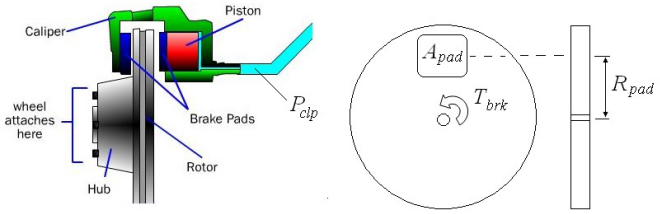

FIGURE 2. SCHEMATIC OF THE DISC BRAKE

A four-wheel vehicle model is employed to simulate the vehicle rigid body dynamics. Fig. 3 shows kinematic and dynamic variables in vehicle and wheel body coordinate frames.

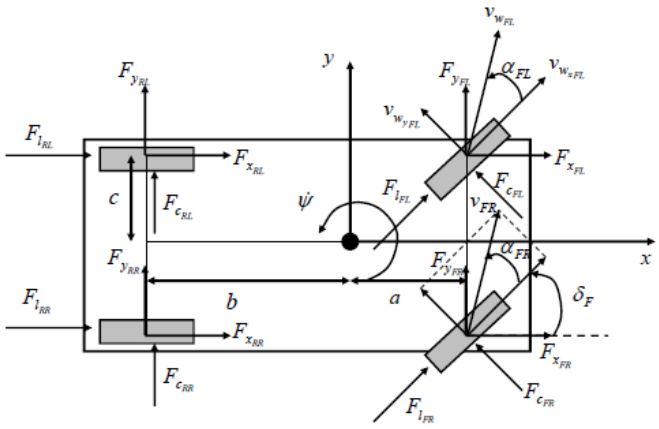

FIGURE 3. TEST VEHICLE

The dynamics equations of motion of a 3-DoF vehicle model are presented in Eq. (4) along with the dynamics equation of the rotating wheels.

$$\begin{Bmatrix} \dot{x} \\ \dot{y} \\ \dot{\psi} \\ \dot{\omega}_{ij} \end{Bmatrix} = \int \begin{Bmatrix} \frac{F_{x\,ij} - F_{drag} - F_{roll}}{m} + \dot{y}\dot{\psi} \\ \frac{F_{y\,ij}}{m} - \dot{x}\dot{\psi} \\ \frac{a}{I_v}\sum F_{y\,Fj} - \frac{b}{I_v}\sum F_{y\,Rj} + \frac{c}{2I_v}\left(\sum F_{x\,iR} - \sum F_{x\,iL}\right) \\ \frac{-T_{Brk\,ij} - F_{Lon\,ij}}{I_w} \end{Bmatrix} dt \tag{4}$$

The velocities of the wheel centers are calculated in the vehicle body coordinate frame and transformed into wheel body frame as presented in Eq. (5).

$$\begin{Bmatrix} v_{wx\,FL} & v_{wx\,FR} \\ v_{wy\,FL} & v_{wy\,FR} \\ v_{wx\,RL} & v_{wx\,RR} \\ v_{wy\,RL} & v_{wy\,RR} \end{Bmatrix} = \begin{bmatrix} \mathbf{R}(\delta_F) & 0 \\ 0 & I \end{bmatrix} \begin{Bmatrix} v_{x\,FL} & v_{x\,FR} \\ v_{y\,FL} & v_{y\,FR} \\ v_{x\,RL} & v_{x\,RR} \\ v_{y\,RL} & v_{y\,RR} \end{Bmatrix}^{vhc}$$
$$= \begin{bmatrix} \cos(\delta_F) & \sin(\delta_F) & 0 & 0 \\ -\sin(\delta_F) & \cos(\delta_F) & 0 & 0 \\ 0 & 0 & 1 & 0 \\ 0 & 0 & 0 & 1 \end{bmatrix} \begin{Bmatrix} \dot{x} - c\dot{\psi} & \dot{x} + c\dot{\psi} \\ \dot{y} + a\dot{\psi} & \dot{y} + a\dot{\psi} \\ \dot{x} - c\dot{\psi} & \dot{x} + c\dot{\psi} \\ \dot{y} - b\dot{\psi} & \dot{y} - b\dot{\psi} \end{Bmatrix} \tag{5}$$

The slip ratio and slip angle of each tire are calculated as presented in Eq. (6) and Eq. (7), respectively, based on the definitions given in [18].

$$\kappa_{ij} = \frac{r\omega_{ij} - v_{l\,ij}}{\max(r\omega_{ij}, v_{l\,ij})} \tag{6}$$

$$\alpha_{ij} = \tan^{-1}\left(\frac{v_{c\,ij}}{v_{l\,ij}}\right) \tag{7}$$

During acceleration/deceleration and cornering maneuvers, the normal tire forces at each tire are estimated by using the dynamic load transfer equations as presented in Eq. (8)

$$\begin{aligned} F_{z\,FL} &= \frac{mgb}{2(a+b)} - \frac{ma_y h}{2c}k_{roll\,F} - \frac{ma_x h}{2(a+b)} \\ F_{z\,FR} &= \frac{mgb}{2(a+b)} + \frac{ma_y h}{2c}k_{roll\,F} - \frac{ma_x h}{2(a+b)} \\ F_{z\,RL} &= \frac{mga}{2(a+b)} - \frac{ma_y h}{2c}k_{roll\,R} + \frac{ma_x h}{2(a+b)} \\ F_{z\,RR} &= \frac{mga}{2(a+b)} + \frac{ma_y h}{2c}k_{roll\,R} + \frac{ma_x h}{2(a+b)} \end{aligned} \tag{8}$$

The tire forces are estimated using longitudinal and lateral Pacejka tire models [21] along with the slip variables, tire-road friction coefficient and normal tire forces at each tire:

$$\begin{aligned} F_{l\,ij} &= f_{Lon}(\kappa_{ij}, \alpha_{ij}, \mu, F_{z\,ij}) \\ F_{c\,ij} &= f_{Lat}(\kappa_{ij}, \alpha_{ij}, \mu, F_{z\,ij}) \end{aligned} \tag{9}$$

Estimated tire forces are transformed back to vehicle coordinate frame using Eq. (10).

$$\begin{Bmatrix} F_{x\,FL} & F_{x\,FR} \\ F_{y\,FL} & F_{y\,FR} \\ F_{x\,RL} & F_{x\,RR} \\ F_{y\,RL} & F_{y\,RR} \end{Bmatrix} = \begin{bmatrix} \mathbf{R}(\delta_F) & 0 \\ 0 & I \end{bmatrix}^{-1} \begin{Bmatrix} F_{l\,FL} & F_{l\,FR} \\ F_{c\,FL} & F_{c\,FR} \\ F_{l\,RL} & F_{l\,RR} \\ F_{c\,RL} & F_{c\,RR} \end{Bmatrix} \tag{10}$$

Observers are designed to estimate vehicle side slip angle and the speed of the vehicle CoG based on the sensor outputs. Vehicle side slip angle is estimated using the accelerometer and yaw rate measurements expressed in inertial frame as presented in Eq. (11) and the details of which are described in [17].

$$\beta = \int \left(-\frac{a}{v_x}\sin(\beta) + \frac{a_y}{v_x} - \dot{\psi} \right) dt \tag{11}$$

Vehicle *CoG* speed is estimated by using either the wheel speeds or the dynamic equations of the rigid body motion according to the driving mode, i.e. acceleration, deceleration, cornering and steady state driving as described in [19].

EXPERIMENTAL VALIDATION OF VEHICLE MODEL

The four wheel vehicle model used in the simulations for the development of the lateral stability control system is verified experimentally. The test vehicle, Alfa Romeo 159, is driven to execute a step change maneuver on an asphalt road with a friction coefficient of 0.9. The initial velocity of the test car is set to 80kph. The steering wheel angle and the brake caliper pressures measured during the tests are used as inputs to the vehicle model, as presented in Fig. 4. Results show that the vehicle model generates similar results as the actual vehicle in terms of the main lateral dynamics outputs of the vehicle, i.e. the lateral acceleration and the yaw rate.

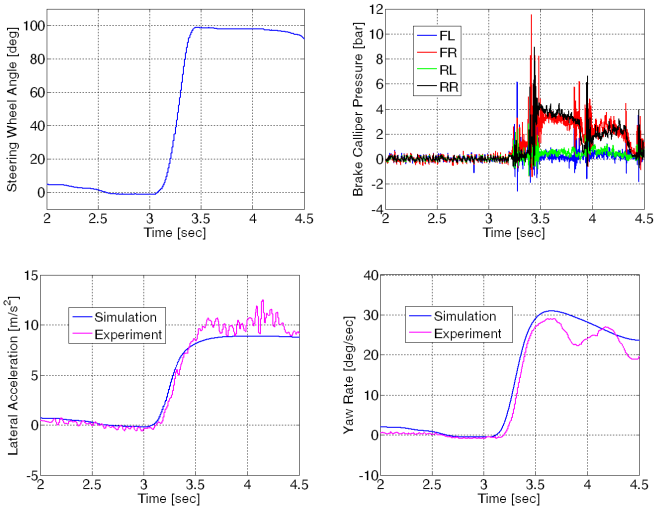

FIGURE 4. VEHICLE MODEL VALIDATION

Since a suspension model is not included in the employed vehicle model, the oscillations of the actual car taking place after 3.5 seconds are not captured by the four wheel model as shown in the yaw rate and the lateral acceleration plots in Fig. 4.

FORCE BASED FEEDBACK CONTROL FOR LOW LEVEL CONTROL SYSTEM

Many passenger vehicles are not equipped with calliper pressure sensors. For this reason the low level controller cannot operate based on calliper pressure feedback. A force based feedback control approach is employed to integrate the HLC and LLC to have a direct feedback from the tire contact patch. Accelerometer based tire sensors can provide an accurate estimation of the longitudinal tire forces by measuring the normal tire forces and the tire-road friction coefficient and using them in the tire models in real-time.

The part of Fig. 1 drawn in dark color represents the closed loop HLC control which generates force requests at every time step, e.g. 50 msec. The part of Fig 1 inside the dotted box represents the closed loop LLC which runs at a faster rate, e.g. 2 msec, and provides the longitudinal forces requested by the HLC.

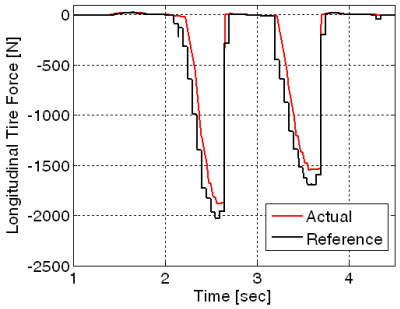

FIGURE 5. FORCE BASED FEEDBACK CONTROL

The performance of the interface based on force feedback is simulated on HIL system and tested on the actual vehicle, as well. A typical performance of the force feedback control approach in a computer simulation is presented in Fig. 5 for the front left wheel of the vehicle during a standard 90/90 maneuver on an asphalt road having a friction coefficient of 0.9. The black curve, in Fig. 5 shows the reference longitudinal tire forces requested by the HLC, whereas the red curve shows the longitudinal force provided by the LLC. An experimental model of the hydraulic brake system is used in this simulation. Results show that the LLC can reliably follow the requests by the HLC.

MEASUREMENT OF TIRE NORMAL FORCE AND FRICITON COEFICENT USING TIRE SENSORS

We use a wireless accelerometer sensor embedded inside the tire to measure the accelerations of viscoelastic tire deformations with respect to the inertial frame. These deformations take place in three different directions, as shown in Fig. 6. [20]

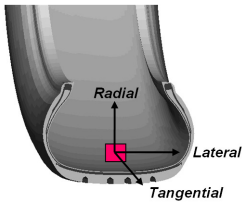

FIGURE 6. COORDINATE SYSTEM FOR THE TIRE

The measured acceleration profiles in the lateral and longitudinal directions can be utilised to estimate the slip variables and horizontal tire forces, whereas the acceleration profiles in the radial direction can be used to estimate the normal forces. By using the estimated variables, the tire-road friction coefficient can also be determined. For the tire-road friction estimation, tire based systems are advantageous compared to vehicle based systems since they could potentially work under steady state operating conditions by measuring small deflections directly from the tire. This simply prevents the load transfer effects of acceleration, deceleration and cornering manoeuvres during the estimation process.

Normal Force Estimation

Radial accelerometer measures the centripetal acceleration as the wheel rotates about its axis. As the sensor approaches to the contact patch, the radial accelerometer also measures the tire deformation due to the reaction forces acting on the carcass from the ground. A typical radial acceleration profile measurement before and after filtering is presented in Fig. 7.

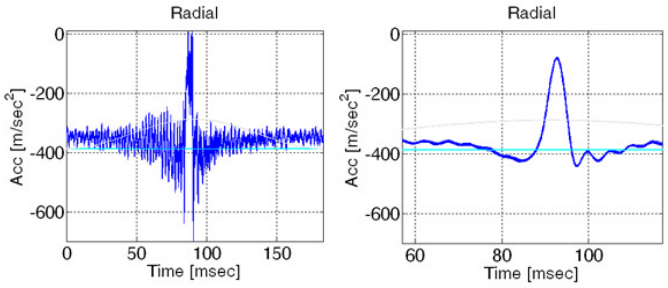

(A) (B)

FIGURE 7. RADIAL ACCELERATION SIGNALS (A) BEFORE AND (B) AFTER LOW PASS FILTERING

One way to estimate the normal forces is to measure the contact patch length in every cycle. If the contact patch is assumed to be perfectly flat and the standing waves on the carcass of the tire are neglected, the accelerometer should measure gravitational acceleration, g in the radial direction once the accelerometer enters the contact patch. This is due to the fact that once inside the tire contact patch, sensor does not move with respect to the ground and stays standstill as the whole wheel body rolls over it. This implies that the portion of the profile having an acceleration of g can be used for the measurement of contact lengths which in turn enable the estimations of normal tire forces by calculating the

maximum vertical deflection ΔR as given in Eq. (4) and using an equivalent nonlinear spring model as shown in Fig. 8.

$$\Delta R = R - \sqrt{R^2 - a^2} \tag{4}$$

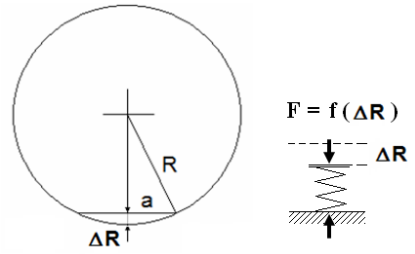

FIGURE 8. MAXIMUM RADIAL DEFLECTION AND NORMAL FORCE ESTIMATION

However, in practice embedded accelerometers are also affected by the vibrations coming from the roadway when they are inside the contact patch. Imperfect filtering process and accelerometer biases also affect the ideal case described in the previous paragraph. Therefore the estimation of the contact length based on the detection of the constant gravitational acceleration is not straightforward.

An alternative practical approach consists of directly correlating the normal tire forces with the width of the low pass filtered *radial* acceleration signal in the vicinity of the peak point as described in [25]. Since the applied normal force changes the contact length and this in turn changes the width of the *radial* acceleration profile, this approach can be used to estimate the normal tire forces. A correlation function between the signal width and the normal force can be formulated for different operating conditions by extensive experimental tests.

Friction Coefficient Estimation

The tire-road friction coefficient is defined as the maximum normalized traction force, i.e. the maximum value of the ratio between the horizontal and normal tire forces as presented in Eq. (5). The horizontal traction force F_H can be represented in terms of lateral, F_x and longitudinal, F_y tire forces [18].

$$\mu := \frac{F_H}{F_V} = \frac{\sqrt{F_x^2 + F_y^2}}{F_V} \tag{5}$$

We propose to estimate the tire-road friction coefficient by using the lateral tire deflection profile. This estimation is based on the measured lateral acceleration profile. The estimation of the tire-road friction coefficient depends on the estimation of the lateral tire force and the slip angle. The lateral tire force is obtained by using a parabolic relationship with the lateral deflections in the contact patch [21]:

$$y_b = \frac{F_y}{2\,c_{bend}} x_b^2 + \frac{M'_z}{c_{yaw}} x_b + \frac{F_y}{c_{lat}} \tag{6}$$

The lateral force F_y and the aligning moment M'_z acting on the tire form the portion of the equatorial line inside the contact patch in three different ways, i.e. shifts this portion in the lateral direction and also yaws and bends it about the normal axis as depicted in Fig. 9.

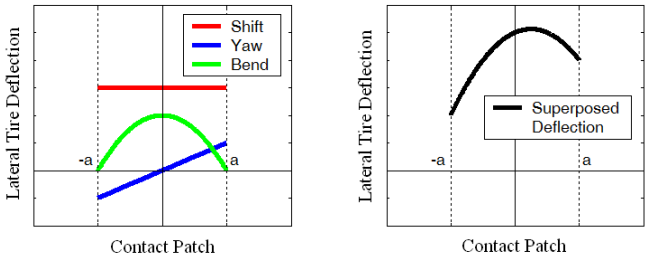

FIGURE 9. JUSTIFICATION OF PARABOLIC FUNCTION

The parabolic function models these three types of deformations by representing the lateral shift, yaw and bending deformations with a constant, a first order and a second order terms, respectively. In other words, the lateral force directly affects the off-set and the slope of the deflection curve through the constant and the second order terms, while the aligning moment gives rise to the asymmetric shape of the curve through the first order term. The coefficients of the parabolic function are assumed to be proportional to the generated lateral force and the aligning moment. The coefficients c_{bend}, c_{yaw} and c_{lat} are known as the proportionality constants used in the model. The tire slip angle is estimated as the slope of the lateral deflection curve at the leading edge of the contact patch [22].

The estimated slip angle and the lateral force are then used in a tire brush model to estimate the tire-road friction coefficient. The proposed friction estimation methodology has been evaluated experimentally in [23] using a piezoelectric tire sensor measuring the uncoupled lateral carcass deflection and promising friction estimation results have been achieved.

The same estimation methodology has been proposed and implemented for accelerometer based tire sensors and preliminary tire-road friction estimation results are also encouraging.

INTEGRATION OF TIRE SENSORS WITH THE VEHICLE STABILITY CONTROL SYSTEM

Accelerometer based tire sensors can be used as a normal tire force sensor and a tire-road friction sensor. The enhanced vehicle stability control system can achieve significantly better performance than a conventional vehicle stability control system if the normal tire force sensor and the tire-road friction sensor are accurate. In fact, traditional vehicle stability control systems use only indirect effect to take into account for the road surface conditions that the vehicle travels on and the amount of current payload that the vehicle carries.

The accelerometer based tire sensors can make a stability control system both road and load adaptive, while increasing its effectiveness in a wide sweep of emergency driving conditions. It also simplifies the control design by requiring less open-loop control action and corresponding involved tuning.

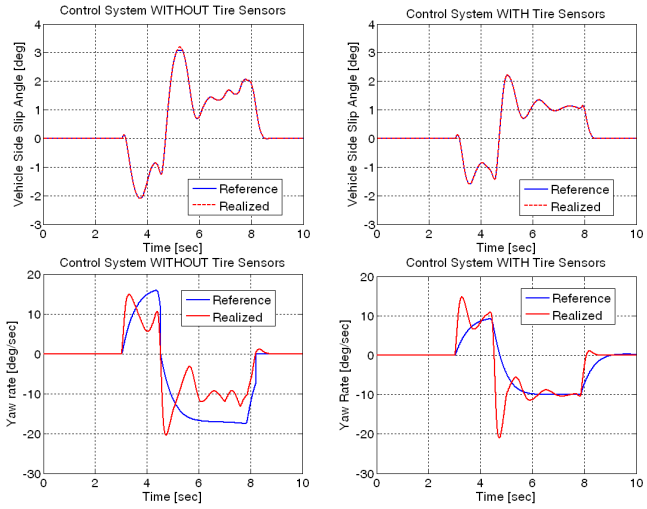

FIGURE 10. ROAD ADAPTIVE SYSTEM PERFORMANCE

The performances of two different control systems are compared. The first controller is a conventional control system which operates on default friction coefficient settings fixed at a nominal value. The second controller is an adaptive control system whose friction coefficient information is updated by the integrated tire sensor measurements. The simulations presented in Fig.10 are executed for a vehicle which is travelling at the speed of 110 [kph] and performing a standard double lane change maneuver (ATI 90/90**)**. The car travels on a roadway with a friction coefficient of 0.3 in both simulations; however one system knows exactly what the friction coefficient is and operates accordingly whereas the other one is set to a nominal value (0.5) and operates indifferent to surface condition changes.

Results show that the knowledge of road surface friction helps the reference generator calculate a better side slip angle and yaw rate reference which eventually leads to a better performance of the adaptive controller. When the tire sensors are available onboard for the measurement of the friction coefficient, the maximum value of the side slip angle decrease about 1^{o} and the vehicle is be able to track the desired yaw rate reliably.

If the tire sensor measures only normal tire forces a load adaptive control system can also be designed when tire sensors are utilized as normal force sensors. The load transfer equations are used to estimate the changes in normal forces on each tire. However, these equations cannot provide any information about the static load change of the vehicle. Tire sensors can be used to estimate the current static normal forces on each tire during a steady state driving.

Figure 11 demonstrates the performance change of the control system when the total mass of the vehicle is increased about 20 percent. These simulations are executed for the same standard double lane change maneuver on dry asphalt having a friction coefficient of 0.9. Static normal tire force information for each tire is assumed to be available to the controller when integrated with the tire sensors. The maximum side slip angle is again decreases more than 1^{o} and the oscillations especially after 5^{th} second are reduced to some degree.

Note that these simulations are executed for our experimental vehicle (a relatively stable sport car) and the benefits can be even higher for less stable vehicles such as commercial vehicles. The simulations clearly represent an upper bound on the potential benefit for the type of vehicle and maneuver considered. We are in the process of validating with experiments the effect of noise and uncertainties on the closed loop behavior.

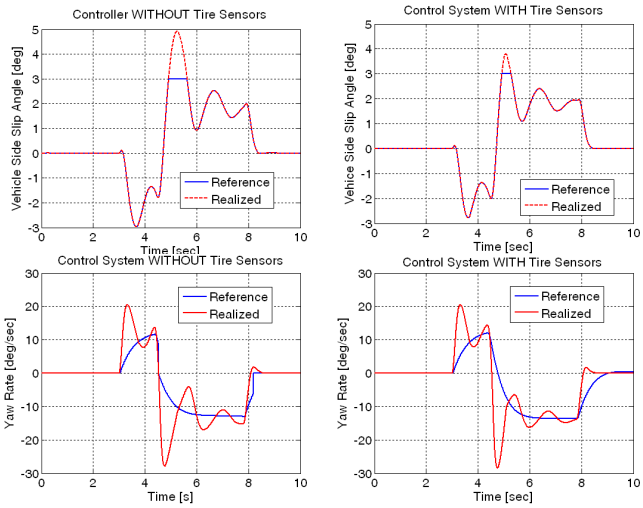

FIGURE 11. LOAD ADAPTIVE SYSTEM PERFORMANCE

CONCLUSIONS

We have presented a hierarchical strategy for designing lateral stability control system which use feedback from accelerometer based tire sensors. We have described the structure of the control system, the integration of the various components and the potential impacts of tire sensors on the design of a lateral stability control system.

In particular accelerometer based tire sensors are proposed to measure the normal tire forces and the tire-road friction coefficient in order to achieve an accurate estimation of the longitudinal tire forces in real time. Preliminary simulation results and HIL tests show that the integrated tire sensors can contribute to the performance of the developed lateral stability control system.

Ongoing research is focused on experimental tests of the integrated smart-tire enabled lateral stability control system and the evaluation of potential benefits on low friction coefficients for a variety of maneuvers.

ACKNOWLEDGMENTS

The authors would like to thank Pirelli Tyre SpA and Politecnico di Torino for the experimental facilities used in this research.

REFERENCES

[1] J. Ackermann, T. Bunte, and D. Odenthal, “Advantages of active steering for vehicle dynamics control,” 1999.

[2] J. Ackermann, “Robust yaw damping of cars with front and rear wheel steering,” in *Proceedings of the 31st Conference on Decision and Control*, Tucson-Arizona, Dec. 1992, pp. 2586–2590.

[3] R. Daily and D. Bevly, “The use of GPS for vehicle stability control systems,” IEEE Transactions on Industrial Electronics, vol. 51, no. 2, pp. 270–277, 2004.

[4] S. Anwar, “Predictive yaw stability control of a brake-by-wire equipped vehicle via eddy current braking,” in *American Control Conference*, 2007, 9-13 July 2007, pp. 2308–2313.

[5] A. T. van Zanten, R. Erthadt, and G. Pfaff, “VDC, the vehicle dynamics control of Bosch,” *in International Congress and Exposition, 1995. Proceeding of the*, ser. SAE950759, March 1995, pp. 9–26.

[6] P. Falcone, F. Borrelli, J. Asgari, H. E. Tseng, and D. Hrovat, “Predictive active steering control for autonomous vehicle systems,” *IEEE Transactions on Control Systems Technology*, vol. 15, no. 3, pp. 566–580, 2007.

[7] G. Palmieri, P. Falcone, H. E. Tseng, and L. Glielmo, “A preliminary study on the effects of roll dynamics in predictive vehicle stability control,” *in Proc. 47th IEEE Conference on Decision and Control CDC 2008*, 9–11 Dec. 2008, pp. 5354–5359.

[8] C. Unsal, and P. Kachroo “Sliding Mode Measurement Feedback Control for Antilock Braking Systems” *IEEE Transactions on Control Systems Technology*, Vol. 7, No. 2, March 1999

[9] D. K. Yoo, L. Wang, “Model based wheel slip control via constrained optimal algorithm” *16th IEEE International Conference on Control Applications Part of IEEE Multi-conference on Systems and Control*, Singapore, 1-3 October 2007

[10] F. Jiang, Z. Gao, “An Application of Nonlinear PID Control to a Class of Truck ABS Problems” *Proceedings of the 40th IEEE Conference on the Decision and Control*, Orlando, Florida Usa, December 2001

[11] Pohl, R. Steindl, L Reindl, 1999 “Intelligent tire utilizing passive SAW sensors - measurement of tire friction”, IEEE Transactions on Instrumentation and Measurement, v 48, n 6, Dec, p 1041-1046

[12] R. Matsuzakia, A. Todoroki, 2005 ”Wireless strain monitoring of tires using electrical capacitance changes with an oscillating circuit” Sensors and Actuators, A 119 323–331

[13] Yilmazoglu, M. Brandt, J. Sigmund, E. Genc, Hartnagele, H.L., 2001 “Integrated InAs/GaSb 3D magnetic field sensors for the intelligent tire”, Sensors and Actuators, A: Physical, v 94, n 1-2, Oct 31, p 59-63

[14] T. Becherer, M. Fehrle, 1996 “Vehicle wheel provided with a pneumatic tire having therein a rubber mixture permeated with magnetizable particles”, US Patent 5895854

[15] Tuononen, A. J., 2008 “Optical position detection to measure tyre carcass deflections”, Vehicle Sys. Dyn.,46:6,471 – 481

[16] S.M. Savaresi, M. Tanelli, P. Langthaler, Luigi Del Re, 2008 “New Regressors for the Identification of Tire Deformation in Road Vehicles via in-tire accelerometers.” IEEE Transactions on Control Systems Tech., Vol. 16, No. 4, pp.769-780, July

[17] U. Kienke and L. Nielsen, Automotive Control Systems. Springer, 2000.

[18] Rajamani, 2006 “Vehicle Dynamics and Control”, ISBN: 978-0-387-26396-0

[19] Mara Tanelli, Sergio M. Savaresi and Carlo Cantoni, “Longitudinal Vehicle Speed Estimation for Traction and Braking Control Systems” Proceedings of the 2006 IEEE International Conference on Control Applications Munich, Germany, October 4-6, 2006

[20] US Patent 7313952 - Method and system for monitoring instantaneous behavior of a tire in a rolling condition

[21] Hans B. Pacejka, 2002 “Tire and Vehicle Dynamics”, Society of Automotive Engineers, Inc.

[22] G. Erdogan, L. Alexander, R. Rajamani, "Novel Wireless Tire Deformation Sensors for Estimation of Slip Angle", *2009 ASME Dynamic Systems and Control Conference*,

[23] G. Erdogan, “New Sensors and Estimation Systems for the Measurement of Tire-Road Friction Coefficient and Tire Slip Variables”, PhD Thesis, University of Minnesota, November 2009

[24] Bosch, Driving-safety systems, Robert Bosch GmbH,1999.

[25] F. Braghin; M. Brusarosco; F. Cheli; A. Cigada; S. Manzoni; F. Mancosu, “Measurement of contact forces and patch features by means of accelerometers fixed inside the tire to improve future car active control” *Vehicle System Dynamics*,Vol. 44, Supplement, 2006, 3–13